OXFORD

BIOLOGY Methods & Protocols

Biology Methods and Protocols, 2025, **10(1),** bpaf021

https://doi.org/10.1093/biomethods/bpaf021
Advance Access Publication Date: 20 March 2025
Methods Article

Mass photometry as a fast, facile characterization tool for direct measurement of mRNA length

Andrew Schmudlach[1,*], Saralynn Spear[1], Yimin Hua[1], Stephanie Fertier-Prizzon[2] and Jianmei Kochling[1]

[1]Analytical Development, mRNA Center of Excellence, Sanofi, Waltham, United States
[2]Analytical Sciences, mRNA Center of Excellence, Sanofi, Marcy l'Etoile, France

*Corresponding author. Analytical Development, mRNA Center of Excellence, Sanofi, Waltham, MA, United States. E-mail: Andrew.schmudlach@sanofi.com

Abstract

Oligonucleotide integrity is a critical quality attribute for many new therapeutic modalities. Current assays often measure attributes such as length using capillary electrophoresis or liquid chromatography. The length is then corroborated with sequencing data to ensure oligonucleotide quality. An orthogonal measure to these classical separations is to measure intact mass, which traditional mass spectrometry cannot. Herein, we report the use of mass photometry to directly measure RNA length using RNA ladders as a calibrant.

Keywords: photometry; facile: characterization; tool; measurements; mRNA

Introduction

New therapeutic modalities have challenged standard analytical workflows derived from older biologics [1–4]. These modalities have included everything from genomic changes using viral vectors to small oligonucleotides delivered in lipid nanoparticles. As our understanding of the underlying biology grows, our questions and analytical techniques need to probe further into the matter. As a case study, large nucleic acid analysis poses challenges due to its overall size, charge, and structure [5–10]. Our current understanding has prioritized certain critical aspects including the presence and percent of mRNA cap modification, the total transcript length, and the presence and length of a polyadenylated tail. Typical analyses for these attributes have relied on a host of different techniques with a focus on chromatographic and electrophoretic separations [11–13]. Some challenges of separations include sample throughput, run time, and detector limitations. Mass spectrometry can complement absorbance-based detectors but has its own shortcomings, including analyte size limitations due to limited m/z windows and generally non-native conditions. Furthermore, separations for size typically employ denaturing conditions to allow for accurate sizing [14]. However, denaturation leads to the loss of information such as the presence of higher order structures and the stoichiometry that may be present [15, 16].

Mass photometry is capable of addressing some of the current challenges in mRNA analytics and provides a useful orthogonality. To begin with, it is capable of providing fast, accurate, and native mass measurements of nucleic acids. Furthermore, mass photometry is not limited to reversed phase ion pairing reagents or volatile salts. Native measurements can be made in a variety of buffers including Tris, phosphate, or citrate with the inclusion of salts. Furthermore, the sensitivity of the technique affords for the analysis of materials in a wide array of matrixes that can be normalized through dilutions.

Mass photometry is a bioanalytical technique that uses light to measure the mass of single biomolecules (including proteins and nucleic acids) in solution [17]. It is based on the principles of interferometric scattering microscopy [18]. Mass photometry has been successfully used to measure the masses of proteins [19], viral particles [20], lipid nanodiscs [21], nucleic acids [22], as well as complexes of these. Mass photometry measurements typically take less than 5 min and use low volumes of sample (≈10 µl) at picomolar to nanomolar concentrations. Measurements have a mass error of ±5%, a resolution of 25 kDa (at 66 kDa), and a mass precision of 2% [17, 23].

Samples measured using mass photometry are placed on a glass slide and illuminated with a laser. The mass photometer then measures the interference between the light scattered by molecules in the sample that land on the measurement surface and the light reflected by the measurement surface. The measured signal, called the mass photometry contrast (or interferometric contrast) depends on the density and refractive index of the particles measured, and it is directly correlated with molecular mass [23]. Since refractive indices and densities vary little within the same class of biomolecule (nucleic acid, protein, etc.), calibration using a molecule of known mass enables mass photometry to be used to measure the mass of other molecules from the same molecular class. Mass photometry can therefore

Received: 13 November 2024; **Revised:** 27 February 2025; **Editorial decision:** 06 March 2025; **Accepted:** 18 March 2025

characterize samples based on the mass distribution of the particles they contain.

Materials and methods

Chemicals/reagents

RiboRuler High Range RNA ladder, urea, phosphate-buffered saline (PBS), 10X TE buffer and 50X TAE electrophoresis buffer were obtained from Thermo Fisher (Waltham, MA, USA). A 25mer standard was purchased from Integrated DNA Technologies (Coralville, IA, USA). 0.5 M sodium citrate buffer pH 6.5 was obtained from TekNova (MansField, MA, USA). All RNA constructs were produced internally at Sanofi's mRNA Center of Excellence (Waltham, MA, USA). Ammonium acetate was sourced from Millipore Sigma (Burlington, MA, USA). P-6 desalting gel columns were obtained from Bio-Rad (Hercules, CA, USA).

Apparatus

TwoMP mass photometer (Refeyn Limited, Oxford, UK). IMgenius ion mobility spectrometer (IonDX Inc., Monterey, CA, USA). PA800 capillary electrophoresis instrument (Sciex, Framingham, MA, USA). 1290 ultra-high-performance liquid chromatography system (Agilent Technologies, Santa Clara, CA, USA). An Xbridge Premier GTx BEH SEC 450Å (4.6 × 150 mm, 2.5 μm) column was obtained from Waters Corp (Milford, MA, USA).

Mass photometry

Refeyn's TwoMP mass photometry system was used to determine the length of mRNA constructs. RiboRuler High Range ladder was used as the standard ladder to which the samples were compared to.

Capillary electrophoresis

Capillary electrophoresis was performed on a Sciex PA800 system and used an eCAP neutral-coated DNA capillary filled with Agilent RNA separation gel. Electric current is applied to the gel allowing the negatively charged mRNA species to move according to size through the gel within the capillary toward a positive electrode Absorbance was set to 254 nm.

Ion mobility

IMgenius was used to determine the inverse mobility constant, or 1/K of mRNAs. IMgenius utilizes an online charge-reducing mechanism to generate singly-charged droplets where the analytes retain their native conformation. Ion mobility spectra of intact mRNAs were processed using the IONBrowser™ software. Samples underwent buffer exchange into ammonium acetate using P-6 desalting gel columns prior to direct infusion.

Size exclusion chromatography

An Xbridge Premier GTx BEH SEC column was installed into an Agilent 1290 UHPLC system with the diode array detector set to record absorbance at 260 nm at a 10 Hz sample rate. Flow rate was set to 0.200 ml/min for all mobile phases. Mobile phases were as indicated in the Supplemental data.

Nano DSC

Constructs 1 and 2 were diluted to 1.00 mg/ml using nuclease free water and transferred into a deep well plate. Samples were introduced to a TA Instruments Nano DSC, and the temperature was increased by 1°C per minute until a temperature of 95°C.

RNA Constructs

Sample	Length (nt)	Poly(A) tail	5′ Cap	Approximate mass (kDa)
Construct 1 IVT	1249	No	No	414.8
Construct 1	1404	Yes	Yes	465.8
Construct 2	2273	Yes	Yes	700.1
Construct 3	2160	Yes	Yes	683.3

Results

Native size measurements of various nucleic acids were tested with RNase free water, 1X PBS, and 1X TE buffer as a diluent for collecting data from the TwoMP system. 1X TE was found to have a higher contrast ratio and was used for subsequent experimentation. The length of the measured nucleic acids agreed was found to be within 5% of orthogonal values. Nucleic acid dimers were observed for Construct 1 when mRNA was diluted in both PBS and TE buffer. The untailed form of Construct 1, which has not undergone enzymatic tailing, Construct 1 IVT, had more dimers when diluted with 1X PBS (Fig. 1). These higher orders structures were found to be noncovalent and reversible through heat denaturation which was also corroborated with orthogonal data (Figs. 2 and 3 and Supplemental data). Mass photometry was shown to be capable of identifying degraded RNA. A single construct was thermally degraded and measured by capillary gel electrophoresis and mass photometry. The data for both showed a decrease in the large, intact mRNA and a corresponding increase in small fragments for degraded samples (Fig. 4 and Table 1). Match-paired untailed and enzymatically tailed mRNA was measured for length by the TwoMP system. Both samples showed accurate length measurements and the difference between the two samples corresponded to the number of adenosines added to the tail during the enzymatic tailing reaction (Fig. 5). Finally, to test the robustness of mass photometry, crude samples from varying stages of the process' workflow were measured. The differences in original salt concentration, buffer concentration, and pH were rendered insignificant and have no discernable impact on length measurements (Fig. 6).

Discussion

To determine what a suitable diluent was for the measurement of RNA using the MP2 mass photometer, we performed dilution measurements on multiple constructs. Our dilution with pure nuclease free water was unsuccessful (Supplemental Fig. 1), however, dilution with 1× PBS and 1× Tris-EDTA (TE) buffers both yielded better results (Fig. 1). Dilution with nuclease free water generated only buffer noise (Supplemental Fig. 1). The failure of the water dilution may be tied to how the RNA is organizing in the absence of buffers or salts. Size exclusion chromatography (SEC) data suggest the formation of higher order species when the analyte is in pure water (Supplemental Fig. 2). This trends with established literature on the impact of ionic strength and the relative size and compaction of single-stranded nucleic acids [24]. The absence of salts influences the RNA into structures that either elute very early in the run or sometimes do not elute at all until a mobile phase with enough salt is introduced. The timescale for the reorganization is very quick as an RNA sample in water can reach an equilibrium between

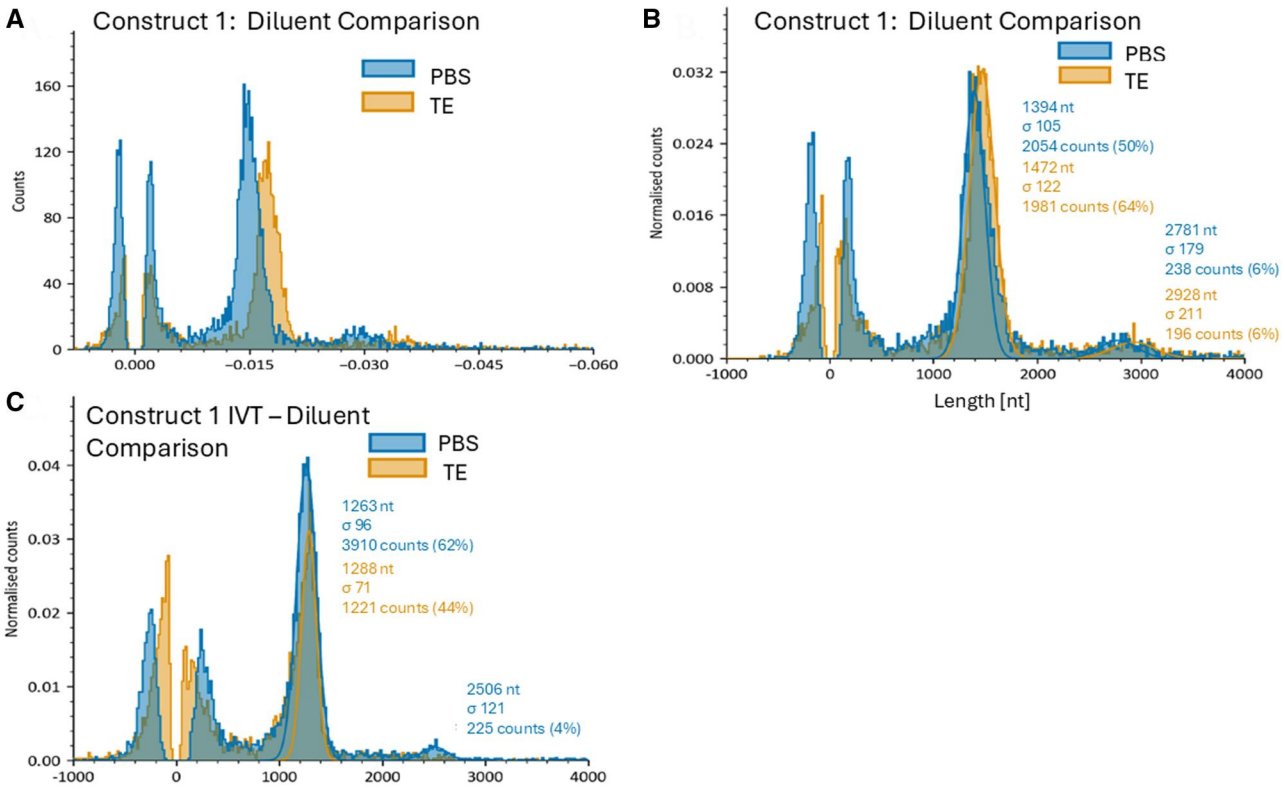

Figure 1. Comparison of mass photometric data with samples diluted in 1× PBS or 1X TE buffer using both ratiometric contrast (A) and length normalized to a standard RNA ladder (B) for Construct 1. The untailed form of Construct 1, Construct 1 IVT, is also compared in 1× PBS and 1× TE buffer (C). Both buffers yielded highly similar length measurements for both the tailed and untailed form of Construct 1; however, TE provided the data over a larger range of ratiometric contract. Subsequent data measurements were performed using TE as the diluent

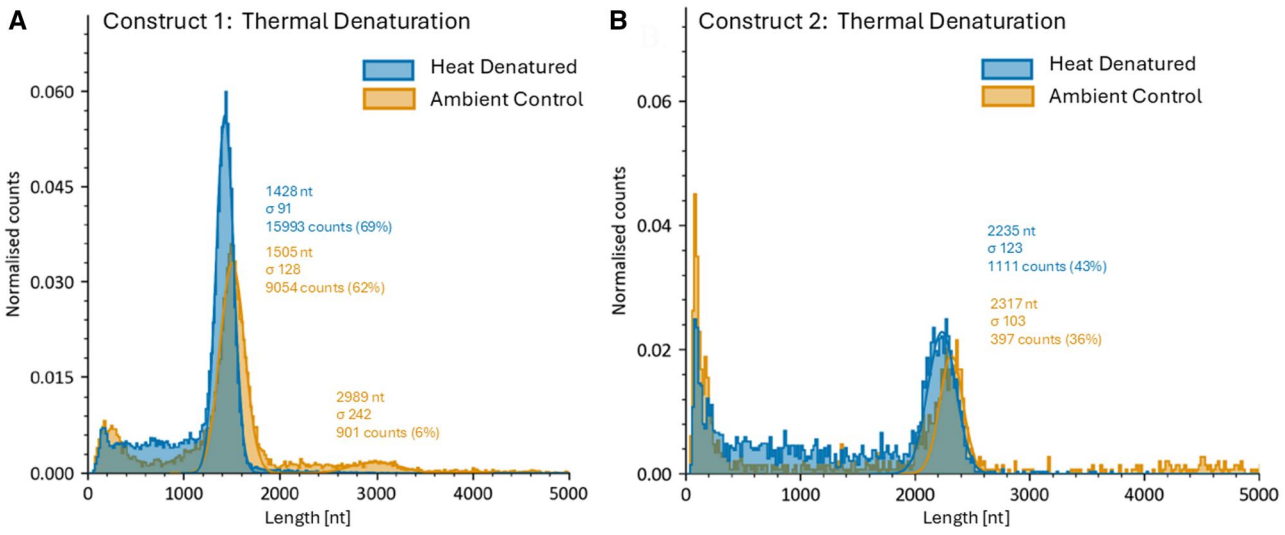

Figure 2. Comparison of mass photometric readouts of Construct 1 (A) and 2 (B) heat denatured at 80°C for 10 min. At ambient temperature in native conditions, the higher-order species are observed, but they are not detected under heat denaturing conditions. This observation can be attributed to the temperature of the sample affecting the measurement because of an altered RI value

monomer and dimer configurations in the time between sample injection and the RNA being introduced into the SEC column. Additional testing using SEC generated data that agreed with current understanding of ionic strength affecting RNA compaction (Supplemental Fig. 3). The failure to generate meaningful data using RNase Free water as a diluent may also be tied to a decreased tendency to adsorb onto the glass slide affecting mass photometric measurements.

The measured lengths of the constructs were very similar for both TE and PBS for Construct 1 (Fig. 1). We observed the same <5% sample measurement from theoretical length for Construct 2 (Fig. 2). Interestingly, we observed the presence of the dimer configuration using PBS as a diluent for Construct 1 IVT sample but not when using the TE buffer. Both diluents yielded dimers when the material was tailed. Of the canonical RNA bases, adenosine is the most hydrophobic. This hydrophobicity may be

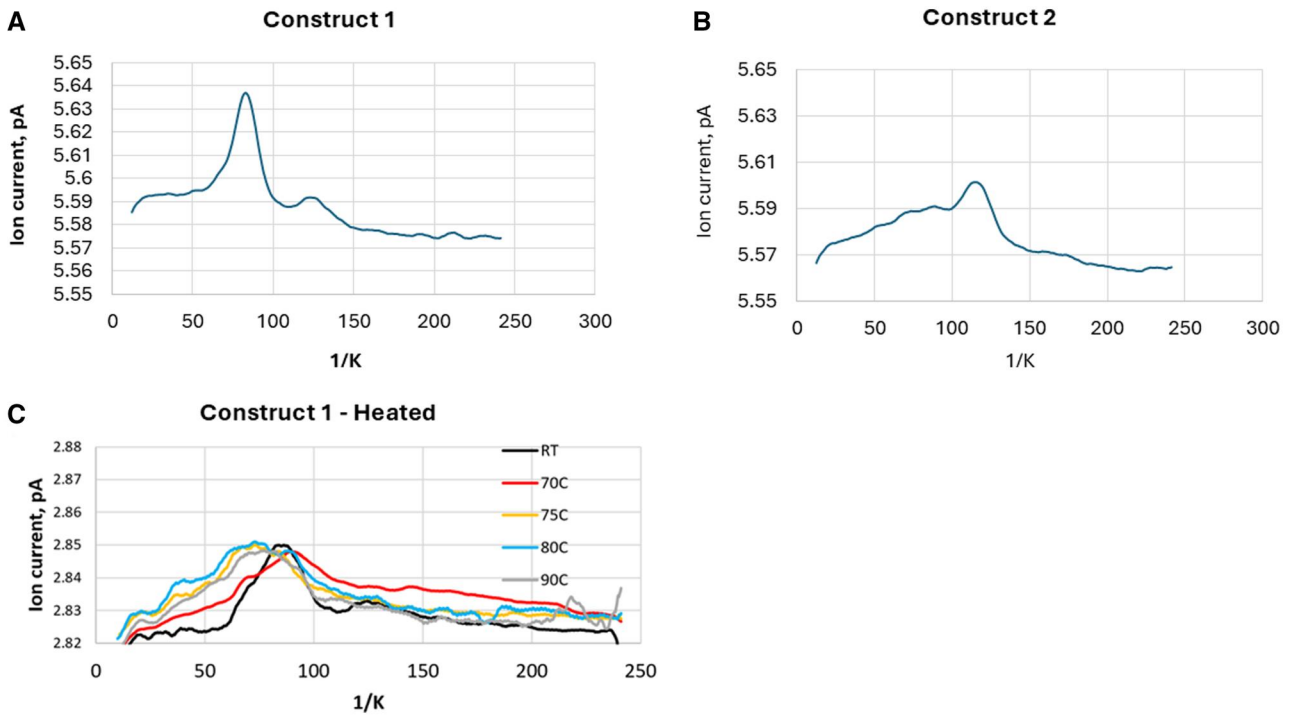

Figure 3. Ion mobilitygrams for the tailed versions of Construct 1 (A), Construct 2 (B), and Construct 1 heated to different temperatures for 10 min (C). Ion mobility was run using ammonium acetate as a buffer as opposed to TE due to the requirement for volatile salts. The presence of higher order species is more pronounced in construct 1 with a much more ordered species present at approximately 125 1/K. These data corroborate the mass photometric data by showing the presence of higher order species

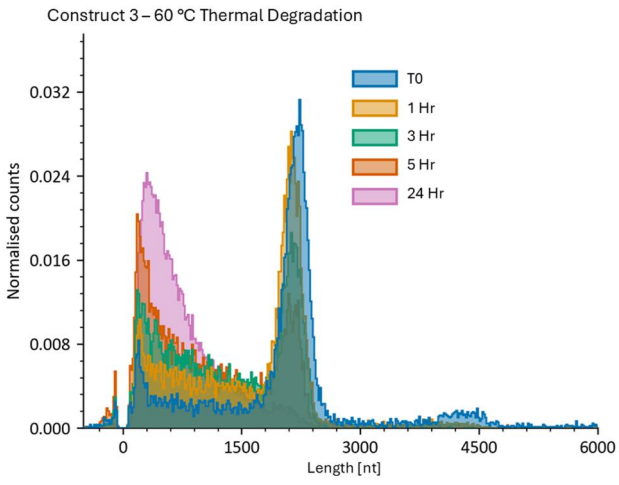

Figure 4. Mass photometric data comparing mRNA Construct 3 degraded at 60°C for 1, 3, 5, and 24 h. Data show a decrease in monomer and higher order species and an increase in the quantity of shorter species

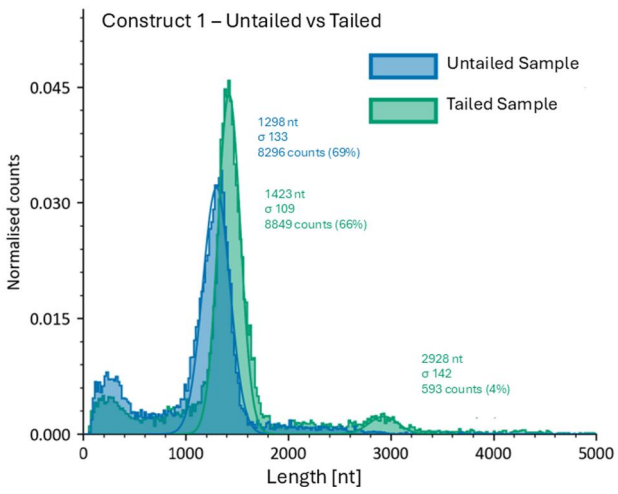

Figure 5. The length of construct 1 enzymatically added poly(A) tail can be measured by the subtraction of the untailed sample length from the tailed sample length. For this instance, a poly(A) tail length of 125 nucleotides was measured which compares to orthogonal measurements. Poly(A) tail length as measured by mass photometry does not give the distribution of the tail, however, the measurement can be determined quickly and with minimal sample handling

Table 1. mRNA integrity measurement as determined by capillary gel electrophoresis for Construct 3 incubated at 60°C for 1, 3, 5, and 24 h. Prolonged incubation is associated with a decline in the mRNA integrity measurement.

Time point	mRNA integrity
T0-Control	75.9
1 h	68.7
3 h	54.7
5 h	44.4
24 h	6.4

driving some of the differences in observed higher order species [14, 15].

Construct 1, in theory, should exist as a more heterogeneous sample compared to Construct 1 IVT as there will be a small distribution of lengths due to the range of sizes produced during the enzymatic tailing process. The approximately 5% difference between the buffers was also observed in both the monomer and dimer species for Construct 2.

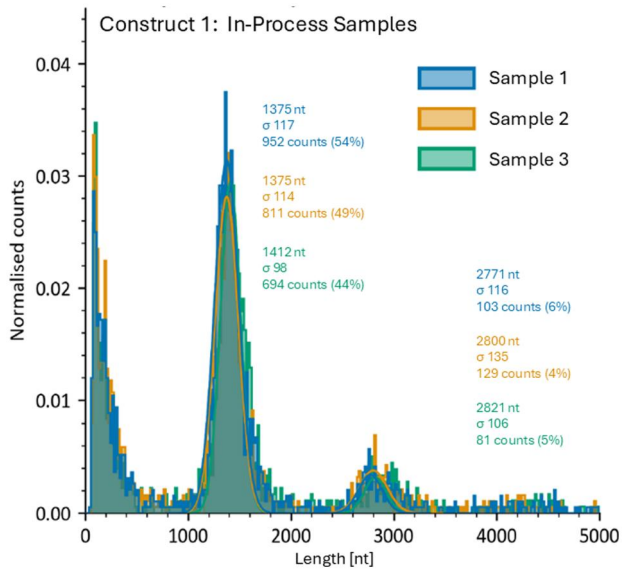

Figure 6. Construct 1 was capped and tailed under varying reaction conditions. The samples were diluted 500X using 1X TE buffer and were measured using the MP2 system. Despite the dissimilar matrix conditions of the original samples, highly reproducible measurements of the samples were possible

Comparing the ratiometric views of Construct 1 tailed vs untailed in TE vs PBS, we observed a greater ratiometric contrast in TE compared to PBS and more pronounced measurements close to 0.00 in PBS. The greater ratiometric contrasts of the TE buffer and the approximately equal accuracy of the size/mass led us to proceed with 1X TE as our diluent of choice.

The observation of higher order species in Constructs 1 and 2 also led us to question whether the higher order structure is reversible. Construct 1 had a higher percent of dimers compared to Construct 2, with a measurable species of approximately 3000 nucleotides. Aliquots of both Construct 1 and 2 were analyzed under ambient conditions and after a 10 min incubation at 80°C [16, 25]. All of the higher order species for these constructs were removed (Fig. 2), demonstrating the reversibility of the higher order structures. Nano DSC determined that 80°C is above the melting temperature of both constructs (Supplemental Figs. 5 and 6). We did observe a shift in the ratiometric contrast of the denatured species compared to the ambient temperature species. This was observed as a shift of 77 and 82 bases for Construct 1 and 2, respectively. It should be noted that the heat-denatured samples were pipetted onto the sample carrier while still hot. The temperature change will result in a change in the refractive index of the sample that likely causes the observed shift, but the observed lengths remain within the expected mass accuracy.

These higher order structures are also observed via an orthogonal native size separation technique: ion mobility. Construct 1's monomer species can be observed at approximately 80 1/K whereas a higher order species is observed at 125 1/K (Fig. 3) [26]. When Construct 1 is incubated at high temperatures for 10 minutes, we observe a reduction of the higher order species. One obvious difference between the two techniques is the fact that the utilized ion mobility instrument requires the use of volatile salts preventing the use of TE buffer. The substitution of one buffer for another could affect the preponderance of higher order species. Given this caveat, we have compelling orthogonal data showing the presence of higher order species which we demonstrate to be reversible using mass photometry.

Measuring intact, high quality nucleic acids is relatively straightforward. Our next investigation probed our ability to measure degradation of Construct 3 after it had been heated for up to 24 h at 60°C. The goal of this incubation was to increase the rate of hydrolysis, thereby reducing RNA integrity [27]. The mass photometric data were compared to electropherograms (Fig. 4, Table 1, and Supplemental Fig. 4). The orthogonal data corroborate with each other with both techniques showing a decrease in main peak and an increase in smaller species. The percent main peak for intact and degraded trended together and showed a reduction of full-length species and a corresponding increase in smaller species but the absolute percent peak areas did not agree. Some of the discrepancy can be attributed to the presence of higher order species observed in mass photometry but not observable in CGE due to denaturation. An additional discrepancy is caused by the buffer interference which is observed as a roughly match-paired measurement at ratiometric contrast close to 0.00. The buffer interference is observed as both positive and negative contrast.

Construct 1 was tailed enzymatically as opposed to being encoded. We sought to determine if an observable difference in mass could be observed between the IVT vs the mature tailed species (Fig. 5). We were able to observe a difference in total mass/length between the tailed and untailed version. Additionally, subtracting the measurements of the IVT from the tailed sample allowed estimating the approximate length of the poly(A) tail. For Construct 1 using mass photometry, we determined the length of the tail to be 125 nucleotides. Interestingly, we were able to observe that the dimer form is much more abundant once Construct 1 was tailed.

A sample matrix study was performed using the crude mid-process samples for Construct 1 (Fig. 6). These samples had various concentrations and species of salt, surfactants, and buffers. These samples reflect the ability to take mass photometry measurements during IVT optimization and process development. All samples were diluted 500× using the same 1× TE buffer. No matrix effects were observed as all three samples had reproducible data outputs for both the monomer and dimer. The dilution factor likely reduced the differences in solution sufficiently to generate reproducible measurements. The monomers lengths were within 3% of each other and the dimer lengths were within 2%. This matrix robustness and overall simplicity of sampling is a large boon for in-process sampling.

Conclusions

Mass photometry has opened up as an orthogonal technique for the sizing of mRNA. Moreover, mass photometry affords native mass measurement which includes details such as higher order structure. The technique worked with both in-process crude samples and purified nucleic acids. The accuracy and precision of mass photometry were found to be within 5% of theoretical and orthogonally measured means. SEC and ion mobility spectroscopy confirmed the presence of higher order structures, their reversibility, and the effects of different diluents on the ratio of these higher order structures in a sample.

Acknowledgements

We would like to acknowledge the assistance and help of Jared Clark, Henry Benner, and Ananya Dubey Kelsoe of IonDX Inc. We would like to acknowledge Refeyn's scientific communications specialist (N. Palanca), brand manager (N. Torres-Tamarit), and

principal scientist (G. Karunanithy) for assistance with preparing the manuscript.

Author contributions

Andrew Schmudlach (Conceptualization [Lead], Data curation [Lead], Formal analysis [Lead], Investigation [Lead], Methodology [Lead], Project administration [Lead], Resources [Supporting], Supervision [Lead], Writing—original draft [Lead]), Saralynn Spear (Formal analysis [Supporting], Investigation [Supporting], Writing—review & editing [Supporting]), Yimin Hua (Project administration [Equal], Resources [Supporting], Supervision [Supporting], Writing—review & editing [Supporting]), and Stephanie Fertier-Prizzon (Project administration [Supporting], Resources [Supporting], Writing—review & editing [Supporting]), and Jianmei Kochling (Project administration [Supporting], Resources [Supporting], Writing—review & editing [Supporting])

Supplementary data

Supplementary data are available at *Biology Methods and Protocols* online.

Conflict of interest statement. All authors are Sanofi employees and may hold shares and/or stock options in the company.

Funding

This work was funded by Sanofi.

Data availability

The data underlying this article are available in the article and in its online supplementary material.

References

1. Fekete S, Doneanu C, Addepalli B. *et al.* Challenges and emerging trends in liquid chromatography-based analyses of MRNA pharmaceuticals. *J Pharm Biomed Anal* 2023;**224**:115174. https://doi.org/10.1016/j.jpba.2022.115174.
2. Ma M, Balasubramanian N, Dodge R. *et al.* Challenges and opportunities in bioanalytical support for gene therapy medicinal product development, *Bioanalysis* 2017;**9**:1423–30. https://doi.org/10.4155/bio-2017-0116.
3. Serrano MAC, Furman R, Chen G. *et al.* Mass spectrometry in gene therapy: challenges and opportunities for AAV analysis. *Drug Discov Today* 2023;**28**:103442. https://doi.org/10.1016/j.drudis.2022.103442.
4. Rosa SS, Prazeres DMF, Azevedo AM. *et al.* MRNA vaccines manufacturing: challenges and bottlenecks. *Vaccine* 2021;**39**:2190–200. https://doi.org/10.1016/j.vaccine.2021.03.038.
5. Kirchner B, Paul V, Riedmaier I. *et al.* MRNA and microrna purity and integrity: the key to success in expression profiling. *Method Mol Biol* 2014;**1160**:43–53. https://doi.org/10.1007/978-1-4939-0733-5_5.
6. Raffaele J, Loughney JW, Rustandi RR. Development of a microchip capillary electrophoresis method for determination of the purity and integrity of MRNA in lipid nanoparticle vaccines. *Electrophoresis* 2022;**43**:1101–6. https://doi.org/10.1002/elps.202100272.
7. Wayment-Steele HK, Kim DS, Choe CA. *et al.* Theoretical basis for stabilizing messenger RNA through secondary structure design. *Nucleic Acids Res* 2021;**49**:10604–17. https://doi.org/10.1093/nar/gkab764.
8. Mauger DM, Cabral BJ, Presnyak V. *et al.* MRNA structure regulates protein expression through changes in functional half-life. *Proc Natl Acad Sci* 2019;**116**:24075–83. https://doi.org/10.1073/pnas.1908052116.
9. Largy E, König A, Ghosh A. *et al.* Mass spectrometry of nucleic acid noncovalent complexes. *Chem Rev* 2022;**122**:7720–839. https://doi.org/10.1021/acs.chemrev.1c00386.
10. Sutton JM, Guimaraes GJ, Annavarapu V. *et al.* Current state of oligonucleotide characterization using liquid chromatography–mass spectrometry: insight into critical issues. *J Am Soc. Mass Spectrom* 2020;**31**:1775–82. https://doi.org/10.1021/jasms.0c00179.
11. Whitley J, Zwolinski C, Denis C. *et al.* Development of mrna manufacturing for vaccines and therapeutics: mrna platform requirements and development of a scalable production process to support early phase clinical trials, *Transl Res* 2022;**242**:38–55. https://doi.org/10.1016/j.trsl.2021.11.009.
12. Wei B, Goyon A, Zhang K. Analysis of therapeutic nucleic acids by capillary electrophoresis. *J. Pharm Biomed Anal* 2022;**219**:114928. https://doi.org/10.1016/j.jpba.2022.114928.
13. Kumar R, Guttman A, Rathore AS. Applications of capillary electrophoresis for biopharmaceutical product characterization. *Electrophoresis* 2022;**43**;143–66. https://doi.org/10.1002/elps.202100182.
14. Shih P, Pedersen LG, Gibbs PR. *et al.* Hydrophobicities of the nucleic acid bases: distribution coefficients from water to cyclohexane 1 1edited by I. Tinoco. *J Mol Biol* 1998;**280**:421–30. https://doi.org/10.1006/jmbi.1998.1880.
15. Gilar M, Fountain KJ, Budman Y. *et al.* Ion-pair reversed-phase high-performance liquid chromatography analysis of oligonucleotides. *J Chromatograph A* 2002;**958**:167–82. https://doi.org/10.1016/s0021-9673(02)00306-0.
16. Kloczewiak M, Banks JM, Jin L. *et al.* A biopharmaceutical perspective on higher-order structure and thermal stability of MRNA vaccines. *Mol Pharm* 2022;**19**:2022–31. https://doi.org/10.1021/acs.molpharmaceut.2c00092.
17. Young G, Hundt N, Cole D. *et al.* Quantitative mass imaging of single biological macromolecules. *Science* 2018;**360**:423–27. https://doi.org/10.1126/science.aar5839.
18. Ortega Arroyo J, Andrecka J, Spillane KM. *et al.* Label-free, all-optical detection, imaging, and tracking of a single protein. *Nano Lett* 2014;**14**:2065–70. https://doi.org/10.1021/nl500234t.
19. Hundt N., Cole D., Hantke M.F.. *et al.* Direct observation of the molecular mechanism underlying protein polymerization. *Sci. Adv* 2022;**8**:eabm7935. https://doi.org/10.1126/sciadv.abm7935.
20. Wagner C, Fuchsberger FF, Innthaler B. *et al.* Quantification of empty, partially filled and full adeno-associated virus vectors using mass photometry. *Int J Mol Sci* 2023;**24**:11033. https://doi.org/10.3390/ijms241311033.
21. Olerinyova A, Sonn Segev A, Gault J. *et al.* Mass photometry of membrane proteins. *Chem* 2020;**14**:224–236.https://doi.org/10.1101/2020.02.28.969287.
22. Li Y, Struwe WB, Kukura P. Single molecule mass photometry of nucleic acids. *Nucleic Acids Res* 2020;**48**:e97. https://doi.org/10.1093/nar/gkaa632.
23. Refeyn TwoMP mass photometer instrument specifications. Refeyn Ltd, http://refeyn.com/twomp

24. Chen H, Meisburger SP, Pabit SA. *et al.* Ionic strength-dependent persistence lengths of single-stranded RNA and DNA. *Proc Natl Acad Sci* 2012;**109**:799–804. https://doi.org/10.1073/pnas.1119057109.
25. Chheda U, Pradeepan S, Esposito E. *et al.* Factors affecting stability of RNA—temperature, length, concentration, ph, and buffering species. *J Pharm Sci* 2024;**113**; 377–85. https://doi.org/10.1016/j.xphs.2023.11.023.
26. Hecht ES, Mehta S, Wecksler AT. *et al.* Insights into ultra-low affinity lipase-antibody noncovalent complex binding mechanisms. *mAbs* 2022;**14**:2135183. https://doi.org/10.1080/19420862.2022.2135183.
27. Becskei A, Rahaman S. The life and death of RNA across temperatures. *Comput Struct Biotechnol J* 2022;**20**:4325–36. https://doi.org/10.1016/j.csbj.2022.08.008.

Biology Methods and Protocols, 2025, 10, 1–7
https://doi.org/10.1093/biomethods/bpaf021
Methods Article